

Article

Solid Energetic Material Based on Aluminum Micropowder Modified by Microwave Radiation

Andrei Mostovshchikov ^{1,2} , Fedor Gubarev ^{3,*} , Pavel Chumerin ¹, Vladimir Arkhipov ⁴, Valery Kuznetsov ⁴ and Yana Dubkova ⁴

¹ School of Nuclear Science & Engineering, National Research Tomsk Polytechnic University, 634050 Tomsk, Russia; avmost@tpu.ru (A.M.); chumerinpy@tpu.ru (P.C.)

² Department of Electronic Technique, Tomsk State University of Control Systems and Radioelectronics, 634050 Tomsk, Russia

³ Research School of Chemistry & Applied Biomedical Sciences, National Research Tomsk Polytechnic University, 634050 Tomsk, Russia

⁴ Scientific Research Institute of Applied Mathematics and Mechanics, National Research Tomsk State University, 634050 Tomsk, Russia; leva@niipmm.tsu.ru (V.A.); dv_1@mail.ru (V.K.); y.a.dubkova@niipmm.tsu.ru (Y.D.)

* Correspondence: gubarevfa@tpu.ru

Abstract: The paper discusses the application of pulsed microwave radiation for the modification of crystalline components of a high-energy material (HEsM). The model aluminized mixture with increased heat of combustion was studied. The mixture contained 15 wt.% aluminum micron powder, which was modified by microwave irradiation. It was found that the HEM thermogram has an exo-effect with the maximum at 364.3 °C. The use of a modified powder in the HEM composition increased the energy release during combustion by 11% from 5.6 kJ/g to 6.2 kJ/g. The reason for this effect is the increase in the reactivity of aluminum powder after microwave irradiation. In this research, we confirmed that the powders do not lose the stored energy, even as part of the HEM produced on their basis. A laser projection imaging system with brightness amplification was used to estimate the speed of combustion front propagation over the material surface. Measurement of the burning rate revealed a slight difference in the burning rates of HEMs based on irradiated and non-irradiated aluminum micropowders. This property can be demanded in practice, allowing a greater release of energy while maintaining the volume of energetic material.

Keywords: aluminum micron powder; microwave radiation; energetic material; aluminized high-energy material; high-speed imaging; laser monitor



Citation: Mostovshchikov, A.; Gubarev, F.; Chumerin, P.; Arkhipov, V.; Kuznetsov, V.; Dubkova, Y. Solid Energetic Material Based on Aluminum Micropowder Modified by Microwave Radiation. *Crystals* **2022**, *12*, 446. <https://doi.org/10.3390/cryst12040446>

Academic Editor: Yang Zhang

Received: 27 February 2022

Accepted: 21 March 2022

Published: 23 March 2022

Publisher's Note: MDPI stays neutral with regard to jurisdictional claims in published maps and institutional affiliations.



Copyright: © 2022 by the authors. Licensee MDPI, Basel, Switzerland. This article is an open access article distributed under the terms and conditions of the Creative Commons Attribution (CC BY) license (<https://creativecommons.org/licenses/by/4.0/>).

1. Introduction

Nowadays, many studies are devoted to investigating aluminum powders and high-energy materials on their basis [1–10]. One of the main research tasks is to increase the specific heat effect of the oxidation of aluminum powders. The solution to this problem is possible with the use of high-energy effects: gamma radiation, neutron flux, electric explosion as a method for producing aluminum nanopowders, etc. [10–12]. An increase in the specific thermal effect of oxidation of metal powders (in particular, aluminum) is explained by the generation and accumulation of defects in the crystal structure of the particles, as well as a change in the configuration of atoms at the grain boundaries and the surface of the particles and is called ‘stored energy’ [11,12]. In particular, in aluminum nanopowders, through such influences, it is possible to increase the specific thermal effect of oxidation by 2.5 kJ/g [13]. In our previous study, we established that aluminum powder significantly increases the thermal oxidation effect (~2.4 kJ/g) after irradiation with the electron beam [14] and exposure to microwave (MW) radiation [15]. The use of MW radiation for these purposes is more expedient and environmentally friendly

due to the relative safety of working with MW radiation, compared to the use of gamma radiation, high-energy electron beams, or neutrons. Other researchers have demonstrated that continuous MW radiation makes it possible to control the combustion process of high-energy materials [16]. At the same time, high-power short-pulse MW radiation makes it possible to generate defects in the crystal structure and on the surface of metal particles but not to ignite them [15]. Such an accumulation of particle structure defects can be useful for their application in high-energy compositions [12,13]. Therefore, it is necessary to determine whether it is possible to improve the energy properties of high-energy materials containing irradiated micron aluminum powders.

The aim of this work is to prove that MW irradiation is effective in increasing the exothermal combustion effect of aluminized energetic material based on aluminum micron powder. At the same time, it is important to understand whether the burning rate of aluminized high-energy material changes when components irradiated with MW radiation are used in its composition. Therefore, the aim of the work is also to estimate the burning rate by visualizing the propagation of the combustion wave front on the surface of the energetic material.

2. Experimental Technique and Material Characteristics

In the experiments, we used the aluminum micron powder produced by spraying liquid aluminum in an inertial medium. The microscopic image of the aluminum micron powder obtained by the JEOL JEM-2100F transmission electron microscope is presented in Figure 1. The particle size distribution was near lognormal with a maximum of 3.5 μm . The particle size distribution was measured using a Shimadzu nanoparticle size distribution analyzer (SALD-7101). The powder contained less than 90 wt.% of active aluminum. The exothermal oxidation effect of the micron powder in air was 5.43 kJ/g; the starting temperature of oxidation was 354.8 $^{\circ}\text{C}$.

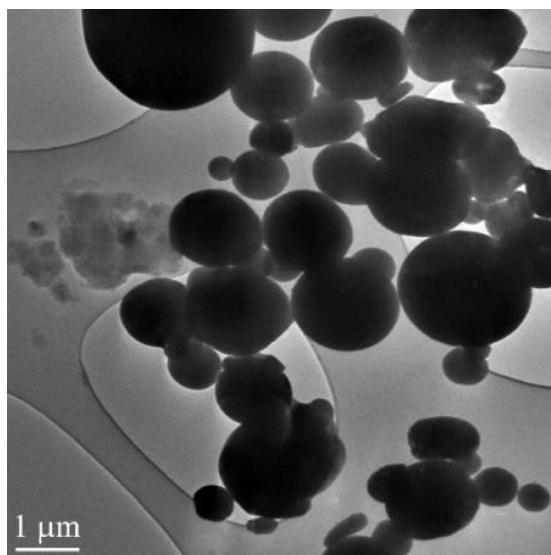


Figure 1. Microscopic image of the aluminum micron powder.

The elementary composition of the micron powder was determined by neutron activation analysis (NAA) [17]. The activation was carried out with a thermal neutrons flux of 5×10^{13} neutrons/ $\text{cm}^2 \cdot \text{s}$ in a 'dry' vertical channel of an IRT-T research nuclear reactor (Tomsk Polytechnic University, Tomsk, Russia). The analysis determined that the powder contained 14 different elements (Table 1). According to Table 1, the total impurity content in the micron powder was lower than 1.6 wt.%. Therefore, the oxidation of impurities did not make a significant contribution to the specific thermal effect of oxidation.

Table 1. Results of neutron activation analysis of aluminum micron powders.

	Element	Content, ($\mu\text{g/g}$)	Standard Enthalpy of Metal Oxidation, $-\text{H}^0$, [kJ/mol]
1	Fe	1127.1934	822.2
2	Ga	265.6707	1089.0
3	Na	114.4161	513.2
4	Zn	32.4767	350.6
5	Cr	11.6218	1140.6
6	Ce	1.9393	125.8
7	Co	1.1021	239.3
8	Mo	0.7081	745.2
9	Sb	0.6379	1007.5
10	Hf	0.2700	1175.5
11	U	0.2449	1224.0
12	W	0.1821	842.9
13	Sc	0.0947	1908.6
14	Sm	0.0493	1822.6

The aluminum micron powder was irradiated by pulsed MW radiation with a frequency of 2.85 GHz and an average power density of 8 kW/cm^2 . The pulse duration was 25 ns and the pulse rate was 400 Hz. The choice of these parameters was due to the requirement that exposure to MW radiation should not lead to sintering or ignition of the powder. Thus, to initiate powder activation processes, a pulsed exposure mode was required, the parameters of which were selected experimentally. The S-band with a frequency exceeding the frequency of household microwave ovens (2.45 GHz), at which the maximum effect on water molecules occurs, was chosen as the frequency range of exposure. The pulse duration and repetition rate were selected experimentally. They were chosen as minimally possible, at which a corona discharge occurs between the particles (Video S1 in Supplementary Materials), but the particles do not sinter and significantly heat up. Irradiation was carried out in air. The powder temperature during irradiation was monitored by an IR camera and did not exceed $40 \text{ }^\circ\text{C}$. Thus, it was insignificant and did not lead to the melting and sintering of the powders. We used the facility for metal powder irradiation in air by MW radiation presented in our previous work [15]. The differential thermal analysis (DTA) [18] of the samples was carried out using an SDT Q600 thermogravimetric analyzer (TA Instruments, New Castle, DE, USA). The experimental study of the burning velocity and combustion heat was conducted to analyze the MW irradiation influence on the burning characteristics of aluminized blended HEM. A similar model composition was used earlier in [8]. The model HEM was obtained by mixing aluminum micron powder with ammonium perchlorate and polymer binder. The mixtures were compacted and dried up. Samples of aluminized blended HEM contained 15.8% inert burning binder (trademark SKDM-80), 69.2% ammonium perchlorate, and 15% non-irradiated aluminum powder (mixture A) and irradiated (mixture B). This percentage composition is optimal for model studies [1]. The cylindrical samples were produced by continuous compaction with a compaction pressure $\sim 2 \times 10^5 \text{ Pa}$. The hardening was carried out for 24 h at a temperature of $20 \text{ }^\circ\text{C}$. The samples were 30–35 mm high and 10 mm in diameter. Their density was $1.70\text{--}0.01 \text{ g}\cdot\text{cm}^{-3}$ and their mass was 1.7–2.0 g.

The complexity of visualizing the surface of burning high-energy materials is caused by the intense glow and scattering of combustion products, which requires the use of the ‘through the flame’ imaging techniques [19,20]. The energetic composition studied in this work belongs to such materials. In the process of combustion, the products scattered, the samples completely lost their shape. The linear burning rate in the air under atmospheric pressure was measured by high-speed laser monitoring. The laser monitor is a laser projection microscope modified with a high-speed camera [21]. The technique of burning rate measurement for aluminum nanopowder mixtures and HEM using high-speed laser monitoring was discussed previously in [20]. Figure 2 presents the laser monitor scheme.

The image in the laser monitor was formed by a system consisting of a concave mirror and a focusing lens, providing a distance to the object of the study equal to 50 cm. The optical scheme allowed us to obtain an observation area with a diameter of ~6 mm and a spatial resolution of 25 μm . The laser monitor was built based on the laboratory-made copper bromide brightness amplifier with a gas-discharge tube aperture of 1.5 cm and a length of the active area of 50 cm. The tube generated 20 μJ pulses of amplified spontaneous emission at 510.6 nm wavelengths and ~0 μJ at 578.2 nm operating at 20 kHz pulse repetition rate [22]. The laser emission of the imaging system had no visible effect on the object of study. The images were recorded using a high-speed digital camera Phantom Miro C110 allowing 900 frms/sec imaging rate with 1280 \times 1024 pixels resolution. The surface area of 4.5 \times 3.6 mm² was visualized.

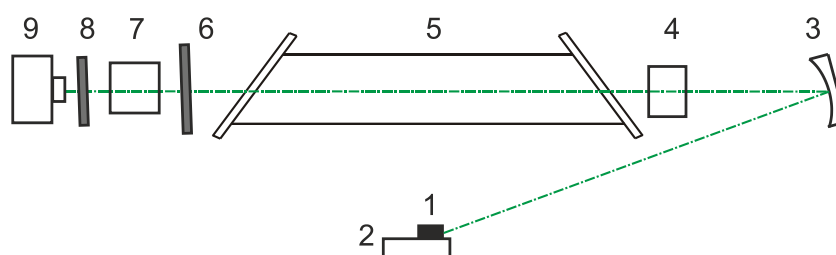


Figure 2. Scheme of the laser monitor. 1—Sample; 2—stage; 3—concave mirror; 4—lens; 5—brightness amplifier; 6 and 8—filters; 7—lens; 9—high-speed camera.

A calorimetric unit in Figure 3 was used to measure the heat of combustion. The sample was placed in a crucible, and then it was burned in the calorimeter-burning chamber, surrounded by water, under an initial oxygen pressure of 2 MPa. Then, the water temperature in the calorimeter chamber was determined. The heat of combustion of the material in the calorimeter-burning chamber was calculated based on the measurement of the water temperature in the calorimeter. The heat of combustion is given by:

$$Q = (C\Delta T \pm \Delta Q)/m \quad (1)$$

where C —the heat capacity of water; ΔT —the change in the water temperature in the calorimetric chamber; ΔQ —the correction factor to take into account the heat exchange with the environment, which characterizes heat losses and does not exceed 1%; and m —the mass of the sample.

The effect of irradiation conditions on the content of metallic Al in the samples was studied by measuring the volume of hydrogen released during the interaction of a powder sample with an alkali solution [23]. The measuring unit consisted of a flask (250 mL), a burette (50 mL) and an equalizing funnel filled with an alkali solution and a saturated NaCl solution, respectively. When Al interacts with an alkali solution, gaseous hydrogen is released, which makes it possible to fix the volume of gas with a burette and calculate the content of metallic Al in the sample from the following chemical reaction:



It has been previously suggested that the change in the thermochemical parameters of aluminum powders after irradiation is associated with the partial destruction of the particle oxide shell. This assumption is confirmed by studies of the MW radiation effect on the structure and phase transitions in aluminum oxide and hydroxide [24–26]. In this work, we carried out model studies on the effect of MW radiation on an amorphous sample of Al oxyhydroxide, which, in its phase composition, imitates the composition of the surface of aluminum powder particles. Al oxyhydroxide was obtained by precipitation from an aqueous mixture of aluminum chloride ($\text{AlCl}_3 \cdot 6\text{H}_2\text{O}$) with an ammonia solution (25%). After that, the precipitate was dried at room temperature for 24 h and then calcined at 250 $^\circ\text{C}$ in air for 4 h.

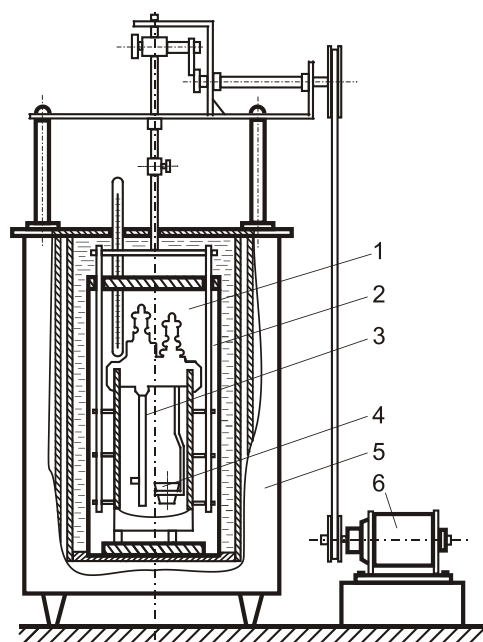


Figure 3. Scheme of the calorimetric unit. 1—Chamber; 2—agitator; 3—ignition device; 4—cruceible with sample; 5—calorimeter body; 6—electric motor.

3. Results and Discussion

We applied a differential thermal analysis to the irradiated samples of the aluminum micron powder that were heated in air up to 1250 °C [14,15,17]. The advantage of the DTA method is the ability to study the state of the oxide layer on the surface of metal particles and determine the dependence of the properties of the particles on the state of the layer [27]. The specific thermal effect of their oxidation was 5.43 kJ/g before MW irradiation. Table 2 presents the DTA results for the irradiated aluminum micron powder with different MW exposure duration. According to the experimental results, the thermal oxidation effect of the aluminum micron powder depends on the time of irradiation. After irradiation for 15 s (optimal), the specific thermal effect of their oxidation increased by 56% and reached 8.48 kJ/g (sample #4). Therefore, sample #4 was chosen for further analyses and model HEM production.

Table 2. Thermochemical characteristics of the aluminum micron powders after pulsed MW irradiation.

	Microwave Exposure Durations	Exothermal Oxidation Effect, kJ/g	Oxidation Start Temperature, °C	Weight Gain Due to Oxidation, %
1	0	5.430	354.85	57.5
2	5	5.391	455.99	58.8
3	10	8.077	405.63	57.8
4	15	8.480	385.31	68.2
5	20	7.156	445.81	61.1
6	25	8.152	443.39	59.4
7	30	7.961	429.72	59.5

The aluminum powder did not change the morphology of the particles after irradiation. The particle size distribution before and after MW irradiation remained virtually unchanged (Figure 4). Aluminum micropowder has a bimodal distribution in the submicron and micron regions. In this case, under MW irradiation, the distribution maximum in the submicron region is shifted towards smaller sizes. This is probably a consequence of the deagglomeration of particles under the action of microwaves.

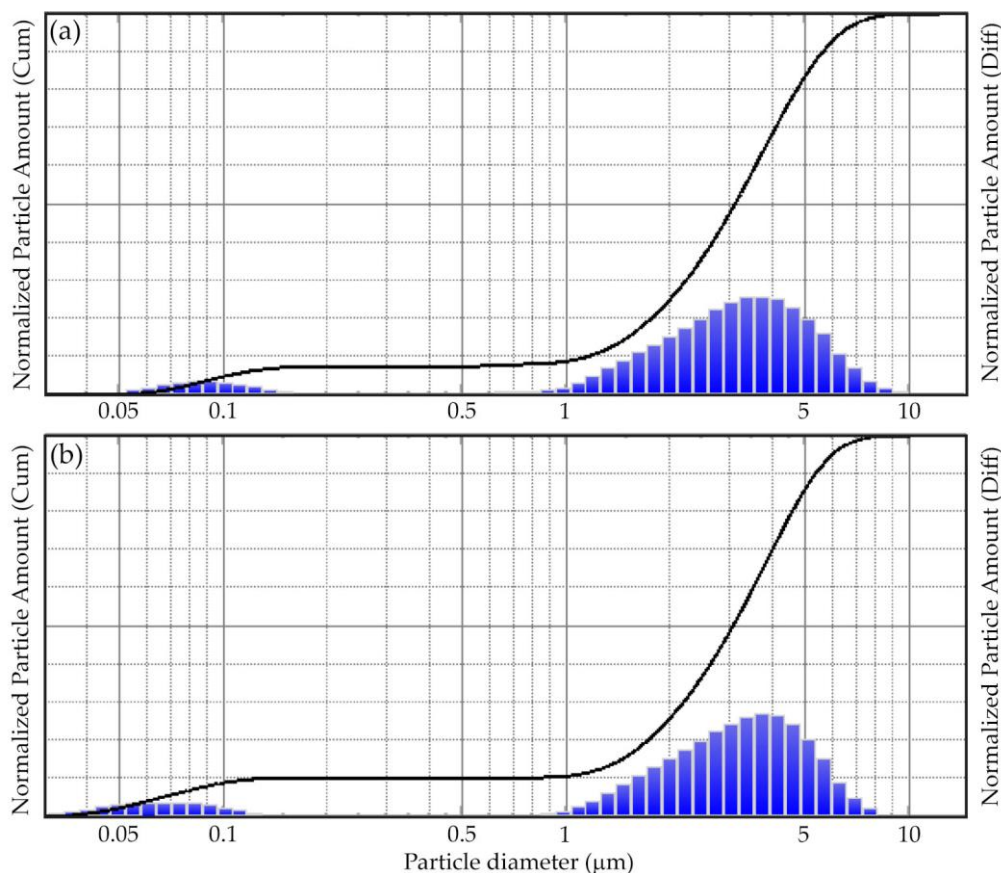


Figure 4. Particle size distributions of non-irradiated (a) and MW irradiated (b) micron powders.

Table 3 presents the results of measurements of the content of metallic aluminum by the volumetric method at different exposure times to MW radiation. The data obtained demonstrate that after exposure to MW radiation, the irradiated samples contained a metallic Al phase, which was absent in the non-irradiated sample. This effect is explained by the reduction of Al oxide in the oxide–hydroxide shell of particles with the formation of metallic Al.

Table 3. Content of metallic aluminum after MW irradiation.

	Microwave Exposure Duration, s	wt. (Al), %
1	0	90.0
2	5	91.0
3	10	91.5
4	15	93.0
5	20	91.5

Figure 5 presents the results of transmission electron microscopy (TEM) of Al oxyhydroxide samples before and after exposure to MW radiation, as well as the electron diffraction patterns of the samples obtained during microscopic examination. As a result of exposure to MW radiation in the amorphous matrix of Al oxyhydroxide, spheroidal structures up to 100 nm in size are formed, which have a higher density compared to the density of the original material. The position of the reflections on the electron diffraction pattern corresponds to the interplanar distances characteristic of the crystal lattice of metallic aluminum. Thus, there is a reviving of metallic aluminum from aluminum oxyhydroxide because of exposure to MW radiation.

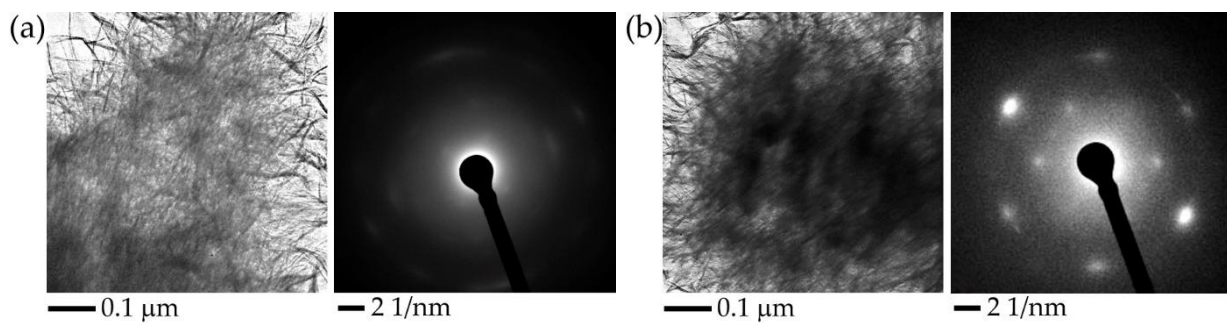


Figure 5. TEM micrographs and electron diffraction patterns of Al oxyhydroxide (a) before and (b) after MW irradiation.

The results of the study of the content of metallic Al and the results of TEM confirm the conclusion that the MW irradiation of aluminum powder increases the reactivity due to an increase in the oxide shell permeability and oxidation rate. Therefore, the partial radiation energy is stored by defects in the particle structure [11,13].

Thermograms of the model HEM were obtained with non-irradiated aluminum micron powder (Figure 6) and the same powder (Figure 7) after MW irradiation in air. According to the DTA results, a sample with irradiated aluminum powder (Figure 7) oxidized much faster than a sample with non-irradiated aluminum (Figure 6) at ~ 300 to 650 °C. This is evidenced by a smoother and more extended exo-effect on the thermogram in Figure 6 (indicated by 1) compared to the ‘needle-like’ exo-effect shape in Figure 7 (indicated by 1). The most likely cause of this ‘needle-like’ shape is the increase in the reactivity of the powder after MW irradiation. A faster oxidation of aluminum particles occurs due to an increase in the permeability of the oxide shell for the oxidizer [15]. In addition, the thermogram of the oxidation of the mixture with irradiated aluminum powder demonstrates the exo-effect in the temperature range from ~ 680 to ~ 1150 °C (indicated by 2). The increase in the heat of oxidation is probably due to a decrease in the agglomeration of the powder, the partial reduction of aluminum in the shell, and an increase in the content of unoxidized aluminum in the powder. This experimentally detected increase in the heat of oxidation after irradiation with short-pulse MW radiation is comparable in magnitude to the effect (~ 2.5 kJ/g) for aluminum nanopowder after irradiation with gamma radiation and electron beams in [13].

The burning rate was studied in this work with the samples of the HEM having the shape of a cylinder with a diameter of 8 mm and a height of 12 mm. The sample was placed horizontally and secured using a mesh form in the central part where there was an observation gap for laser monitoring, similar to work [20]. Figure 8 presents the frames of high-speed imaging obtained for non-irradiated aluminum micron powder combustion. Combustion was initiated with the gas burner; therefore, it was not possible to register the exact moment of ignition. The operator triggered the camera recording when a visible flame appeared.

The use of a laser monitor makes it possible to observe the surface of the sample during combustion. Despite the high brightness and scattering of combustion products, the laser monitor successfully records the changes in the sample surface. In particular, we can clearly monitor the propagation of the burning front and estimate its rate using this imaging technique. The visible combustion front clearly separates the homogeneous surface of the source material from the inhomogeneous surface of the burning material. The arrows and dotted lines mark the position of the burning front during combustion. For the edges’ identification, we varied the brightness and contrast of the images converted to the gray scale and compared neighboring pixels. This approach was sufficient for determining the front position with an accuracy of 5–10 pixels.

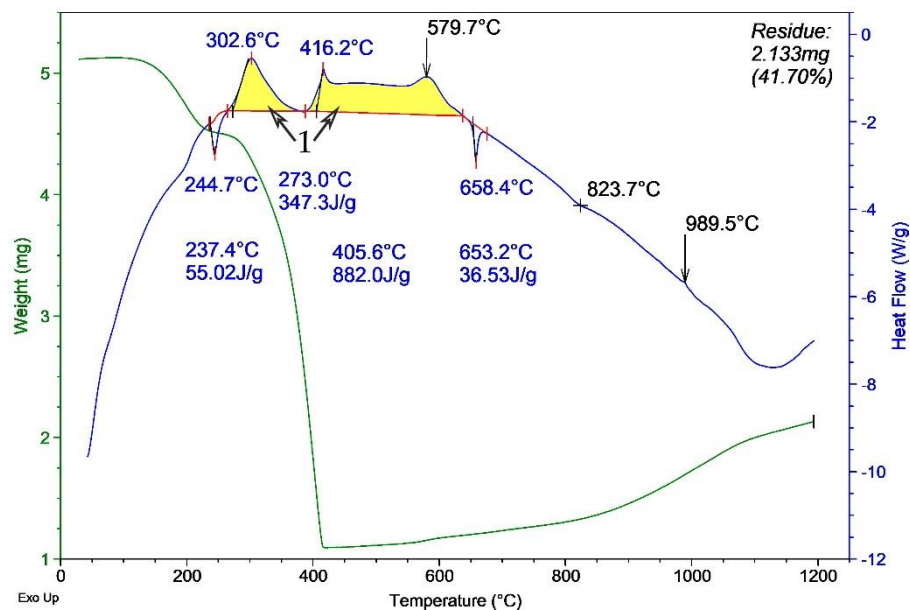


Figure 6. Thermogram of the model HEM obtained with non-irradiated aluminum micron powder (heating rate is 10 °C/min in air). 1—exo-effect.

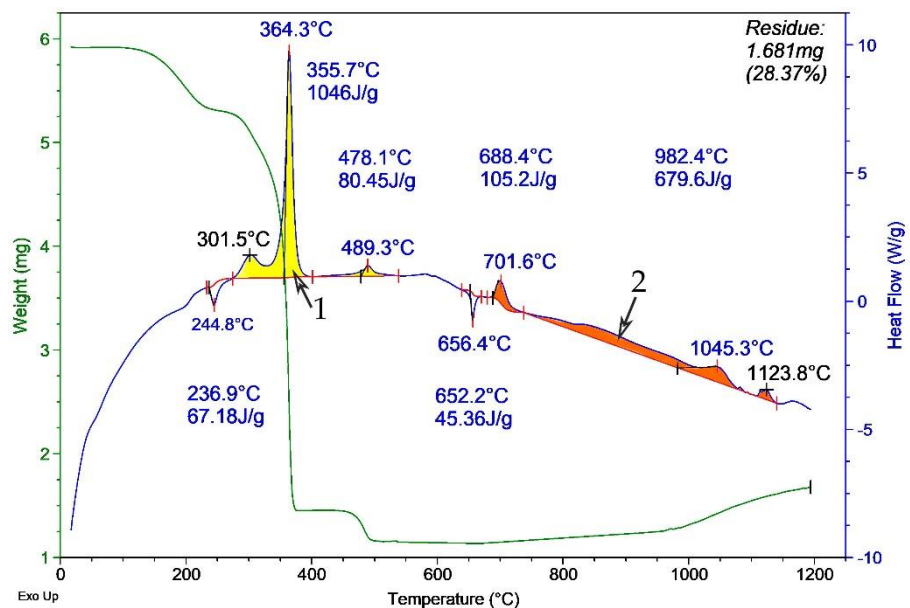


Figure 7. Thermogram of the model HEM obtained with irradiated aluminum micron powder (heating rate is 10 °C/min in air). 1, 2—exo-effects.

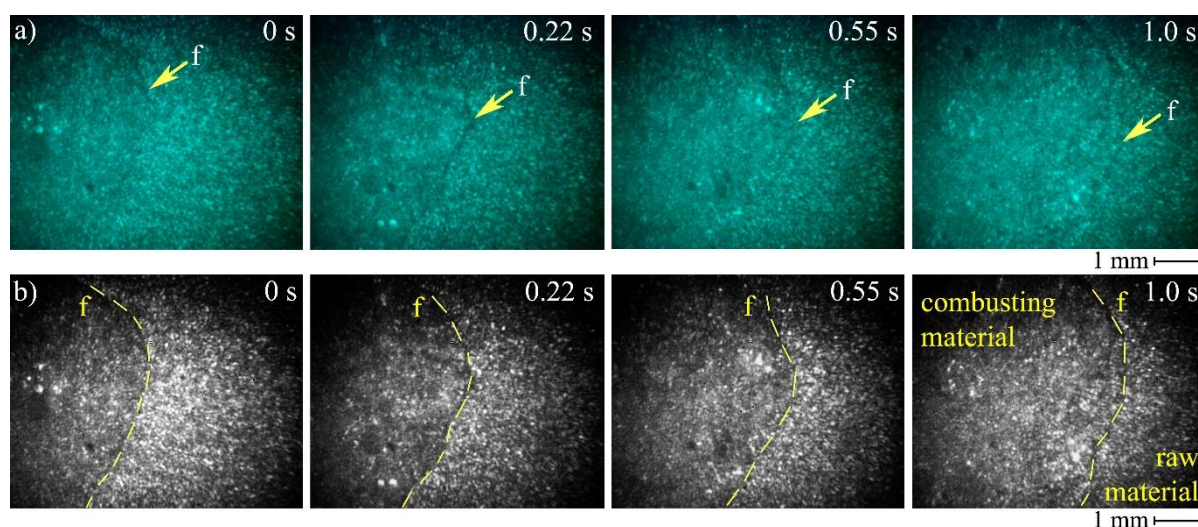


Figure 8. Frames of high-speed imaging of non-irradiated aluminum micron powder combustion: (a) original frames at different moments of time during combustion; (b) gray scale representation of the same images with brightness/contrast fitting; f—current position of the burning front.

Table 4 presents the results of the burning rate measurement using high-speed imaging with the laser monitor. Six samples with the same size were under the study. The measurement of the burning rate using a laser speed imaging system demonstrated a slight difference in the burning rate of HEMs based on irradiated and non-irradiated aluminum micropowder.

Table 4. The burning rate of the samples.

The Initial Temperature of the Sample, °C	Type of the Composition	Average Burning Rate, mm/s
20	A (non-irradiated)	1.57 ± 0.04
	B (irradiated)	1.52 ± 0.03

Table 5 presents the results of the combustion heat measurement. The analysis of measurement results demonstrates that the irradiated samples (group B) have 11% higher combustion heat than the non-irradiated samples (group A). The energy release of the HEM with irradiated powder reached 6.2 kJ/g. However, the burning rate did not depend on the type of aluminum powder (non-irradiated or irradiated).

Table 5. The combustion heat of the HEM samples.

Group	Q, kJ/g
Group A (non-irradiated)	5.6 ± 0.1
Group B (irradiated)	6.2 ± 0.1

According to the data in Tables 4 and 5, the use of irradiated aluminum micropowder in the composition of HEM allows the increase in the energy of combustion of the material, while maintaining an unchanged combustion rate. This is necessary for those applications when it is required to increase the heat release in mixtures while maintaining the same speed of the technological process or the volume of reagents (for example, for welding thermites, fuel compositions, etc.).

4. Conclusions

This work proved the results of our earlier study [15] that discovered that irradiated powders were capable of storing the radiation energy due to an increase in the surface

charge of metal particles, thus increasing their reactivity. This assumption is theoretically confirmed by [28], which demonstrates that the microwave field in nanoparticles is absorbed not only by the core of the nanoparticles but also by the oxide shell of the nanoparticles. We achieved this effect in metal micron particles using short-pulse microwave radiation, in contrast to the works of other researchers who observed a similar effect using hard radiation: high-energy electrons, gamma rays, or neutrons. Exothermal oxidation effect increased from 5.43 to 8.48 kJ/g (by 1.56 times) when irradiated with a frequency of 2.85 GHz, an average power density of 8 kW/cm², a pulse duration of 25 ns, and a pulse rate of 400 Hz during 15 s.

In this work, based on the study of aluminum micropowder, we confirm that the stored energy during the irradiation of the initial micropowder is not lost when the micropowder becomes part of the high-energy mixture. The heat of combustion of the modified aluminized model composition in the bomb calorimeter increased by 11% (or 0.6 kJ/g) from 5.6 kJ/g for non-irradiated to 6.2 kJ/g for MW irradiated micropowder. Meanwhile, the burning velocity does not depend on the type of powder used in the HEM composition (microwave-irradiated or non-irradiated). Therefore, the application of the irradiated Al micron powder could improve the exothermal characteristics of the HEM without compromising the linear burning rate.

Supplementary Materials: The following supporting information can be downloaded at: <https://www.mdpi.com/article/10.3390/cryst12040446/s1>, Video S1: Video of the process of exposure to microwave radiation. The micropowder is placed in a glass vessel, which is placed in the window of the microwave waveguide. During exposure, a blue glow is observed.

Author Contributions: Conceptualization, A.M., F.G. and V.A.; methodology, A.M., F.G., V.A. and V.K.; software, F.G.; validation, V.K. and Y.D.; formal analysis, P.C.; investigation, A.M., F.G. and Y.D.; resources, A.M., P.C. and V.A.; data curation, A.M. and V.K.; writing—original draft preparation, A.M. and F.G.; writing—review and editing, A.M. and F.G.; visualization, F.G.; supervision, P.C. and V.A.; project administration, A.M.; funding acquisition, A.M. and P.C. All authors have read and agreed to the published version of the manuscript.

Funding: This research received no external funding.

Data Availability Statement: The data presented in this study are available on request from the corresponding author.

Acknowledgments: This research was supported by the Tomsk Polytechnic University development program and Tomsk State University competitiveness improvement program.

Conflicts of Interest: The authors declare no conflict of interest.

References

1. Ellern, H. *Military and Civilian Pyrotechnics*; Chemical Publisher Company Inc.: New York, NY, USA, 1968.
2. Beckstead, M.W. A summary of aluminium combustion. In Proceedings of the RTO/VKI Special Course on “Internal Aerodynamics in Solid Rocket Propulsion”, Rhode-Saint-Genèse, Belgium, 27–31 May 2002.
3. Ivanov, Y.F.; Osmonoliev, M.N.; Sedoi, V.S.; Arkhipov, V.A.; Bondarchuk, S.S.; Vorozhtsov, A.B.; Korotkikh, A.G.; Kuznetsov, V.T. Productions of ultra-fine powders and their use in high energetic compositions. *Propellants Explos. Pyrotech.* **2003**, *28*, 319–333. [[CrossRef](#)]
4. Teipel, U. *Energetic Materials*; Wiley-VCH: Weinheim, Germany, 2004.
5. Mullen, J.C.; Brewster, M.Q. Reduced agglomeration of aluminum in wide-distribution composite propellants. *J. Propuls. Power* **2011**, *27*, 650–661. [[CrossRef](#)]
6. Brewster, M.Q.; Mullen, J.C. Burning-rate behavior in aluminized wide-distribution AP composite propellants. *Combust. Explos. Shock Waves* **2011**, *47*, 200–208. [[CrossRef](#)]
7. Wang, F.; Wu, Z.; Shangguan, X.; Sun, Y.; Feng, J.; Li, Z.; Chen, L.; Zuo, S.; Zhuo, R.; Yan, P. Preparation of mono-dispersed, high energy release, core/shell structure Al nanopowders and their application in HTPB propellant as combustion enhancers. *Sci. Rep.* **2017**, *7*, 5228. [[CrossRef](#)] [[PubMed](#)]
8. Korotkikh, A.G.; Glotov, O.G.; Arkhipov, V.A.; Zarko, V.E.; Kiskin, A.B. Effect of iron and boron ultrafine powders on combustion of aluminized solid propellants. *Combust. Flame* **2017**, *178*, 195–204. [[CrossRef](#)]

9. Nguyen, Q.; Huang, C.; Schoenitz, M.; Sullivan, K.T.; Dreizin, E.L. Nanocomposite thermite powders with improved flowability prepared by mechanical milling. *Powder Technol.* **2018**, *327*, 368–380. [[CrossRef](#)]
10. Balaji, A.B.; Ratnam, C.T.; Khalid, M.; Walvekar, R. Effect of electron beam irradiation on thermal and crystallization behavior of PP/EPDM blend. *Radiat. Phys. Chem.* **2017**, *141*, 179–189. [[CrossRef](#)]
11. Ivanov, G.V.; Tepper, F. 'Activated' aluminum as a stored energy source for propellants. *Int. J. Energet. Mater. Chem. Propuls.* **1997**, *4*, 636–645.
12. Kuo, K.K.; Acharya, R. *Applications of Turbulent and Multiphase Combustion*; John Wiley & Sons: Hoboken, NJ, USA, 2012.
13. Kuo, K.K.; Risha, G.A.; Evans, B.J.; Boyer, E. Potential usage of energetic nano-sized powders for combustion and rocket propulsion. *MRS Online Proc. Libr.* **2003**, *800*, 3–14. [[CrossRef](#)]
14. Mostovshchikov, A.V.; Ilyin, A.P.; Egorov, I.S. Effect of electron beam irradiation on the thermal properties of the aluminum nanopowder. *Radiat. Phys. Chem.* **2018**, *153*, 156–158. [[CrossRef](#)]
15. Mostovshchikov, A.V.; Il'in, A.P.; Chumerin, P.Y.; Yushkov, Y.G. Parameters of iron and aluminum nano- and micropowder activity upon oxidation in air under microwave irradiation. *Tech. Phys.* **2018**, *63*, 1223–1227. [[CrossRef](#)]
16. Barkley, S.J.; Zhu, K.; Lynch, J.E.; Michael, J.B.; Sippel, T.R. Microwave plasma enhancement of multiphase flames: On-demand control of solid propellant burning rate. *Combust. Flame* **2019**, *199*, 14–23. [[CrossRef](#)]
17. Moreira, E.G.; Vasconcellos, M.B.A.; Saiki, M. Uncertainty assessment in instrumental neutron activation analysis of biological materials. *J. Radioanal. Nucl. Chem.* **2006**, *269*, 377–382. [[CrossRef](#)]
18. Wendlandt, W.W. *Thermal Methods of Analysis*, 2nd ed.; John Wiley & Sons: New York, NY, USA, 1974.
19. Zepper, E.T.; Pantoya, M.L.; Bhattacharya, S.; Marston, J.O.; Neuber, A.A.; Heaps, R.J. Peering through the flames: Imaging techniques for reacting aluminum powders. *Appl. Opt.* **2017**, *56*, 2535–2541. [[CrossRef](#)] [[PubMed](#)]
20. Li, L.; Mostovshchikov, A.V.; Ilyin, A.P.; Antipov, P.A.; Shiyanov, D.V.; Gubarev, F.A. Gubarev, In Situ nanopowder combustion visualization using laser systems with brightness amplification. *Proc. Combust. Inst.* **2021**, *38*, 1695–1702. [[CrossRef](#)]
21. Evtushenko, G.S. *Methods and Instruments for Visual and Optical Diagnostics of Objects and Fast Processes*; Nova Science Publishers: New York, NY, USA, 2018.
22. Li, L.; Shiyanov, D.V.; Gubarev, F.A. Spatial-temporal radiation distribution in a CuBr vapor brightness amplifier in a real laser monitor scheme. *Appl. Phys. B Lasers Opt.* **2020**, *126*, 155. [[CrossRef](#)]
23. Korshunov, A.V.; Yosypchuk, B.; Heyrovský, M. Voltammetry of aqueous chloroauric acid with hanging mercury drop electrode. *Coll. Czech. Chem. Commun.* **2011**, *76*, 929–936. [[CrossRef](#)]
24. Standish, N.; Worner, H. Microwave application in the reduction of metal oxides with carbon. *J. Microw. Power Electromagn. Energy* **1990**, *25*, 177–180. [[CrossRef](#)]
25. Jung, Y.H.; Jang, S.O.; You, H.J. Hydrogen generation from the dissociation of water using microwave plasmas. *Chin. Phys. Lett.* **2013**, *30*, 065204. [[CrossRef](#)]
26. Lu, Y.-H.; Chen, H.-T. Hydrogen generation by the reaction of H₂O with Al₂O₃-based materials: A computational analysis. *Phys. Chem. Chem. Phys.* **2015**, *17*, 6834. [[CrossRef](#)]
27. Pisharath, S.; Fan, Z.; Ghee, A.H. Influence of passivation on ageing of nano-aluminum: Heat flux calorimetry and microstructural studies. *Thermochim. Acta* **2016**, *635*, 59–69. [[CrossRef](#)]
28. Biswas, P.; Mulholland, G.W.; Rehwoldt, M.C.; Kline, D.J.; Zachariah, M.R. Microwave absorption by small dielectric and semi-conductor coated metal particles. *J. Quant. Spectrosc. Radiat. Transf.* **2020**, *247*, 106938. [[CrossRef](#)]